Results on $\nu_\mu \rightarrow \nu_e$ Neutrino Oscillations from the LSND Experiment

C. Athanassopoulos,[11] L. B. Auerbach,[11] R. L. Burman,[6] D. O. Caldwell,[3] E. D. Church,[1] I. Cohen,[5] J. B. Donahue,[6]
A. Fazely,[10] F. J. Federspiel,[6] G. T. Garvey,[6] R. M. Gunasingha,[7] R. Imlay,[7] K. Johnston,[8] H. J. Kim,[7] W. C. Louis,[6]
R. Majkic,[11] K. McIlhany,[1] G. B. Mills,[7] R. A. Reeder,[9] V. Sandberg,[6] D. Smith,[4] I. Stancu,[1] W. Strossman,[1]
R. Tayloe,[6] G. J. VanDalen,[1] W. Vernon,[2] N. Wadia,[7] J. Waltz,[4] D. H. White,[6] D. Works,[11] Y. Xiao,[11] and S. Yellin[3]

(LSND Collaboration)

[1]*University of California, Riverside, California 92521*
[2]*University of California, San Diego, California 92093*
[3]*University of California, Santa Barbara, California 93106*
[4]*Embry Riddle Aeronautical University, Prescott, Arizona 86301*
[5]*Linfield College, McMinnville, Oregon 97128*
[6]*Los Alamos National Laboratory, Los Alamos, New Mexico 87545*
[7]*Louisiana State University, Baton Rouge, Louisiana 70803*
[8]*Louisiana Tech University, Ruston, Louisiana 71272*
[9]*University of New Mexico, Albuquerque, New Mexico 87131*
[10]*Southern University, Baton Rouge, Louisiana 70813*
[11]*Temple University, Philadelphia, Pennsylvania 19122*
(Received 10 September 1997)

A search for $\nu_\mu \rightarrow \nu_e$ oscillations has been conducted with the LSND apparatus using ν_μ from π^+ decay in flight. Two analyses observe a total of 40 beam-on high-energy (60–200 MeV) electron events consistent with the $\nu_e C \rightarrow e^- X$ inclusive reaction. This number is significantly above the 21.9 ± 2.1 events expected from the ν_e contamination in the beam and the beam-off background. If interpreted as an oscillation signal, the observed oscillation probability of $(2.6 \pm 1.0 \pm 0.5) \times 10^{-3}$ is consistent with the previously reported $\overline{\nu}_\mu \rightarrow \overline{\nu}_e$ oscillation evidence from LSND. [S0031-9007(98)06970-1]

In this Letter we describe the results of a search for $\nu_\mu \rightarrow \nu_e$ oscillations using a ν_μ flux from π^+ decay in flight (DIF). The data were taken with the Liquid Scintillator Neutrino Detector (LSND) at the Los Alamos Meson Physics Facility (LAMPF). The result of a search for $\overline{\nu}_\mu \rightarrow \overline{\nu}_e$ oscillations, using a $\overline{\nu}_\mu$ flux from μ^+ decay at rest (DAR), has already been reported in Ref. [1], where an excess of events was interpreted as evidence for neutrino oscillations. The analysis presented here uses a different component of the neutrino beam, a different detection process, and has different backgrounds and systematics from the previous DAR result, providing a consistency check on the existence of neutrino oscillations.

The primary source of DIF ν_μ for this experiment is the A6 water target of the LAMPF 800 MeV proton linear accelerator. Approximately 3.4% of the π^+ produced in the 30-cm-long target decay in flight before reaching the water-cooled copper beam stop, situated 1.5 m downstream. The generated ν_μ flux is illustrated in Fig. 1(a), as calculated at the center of the detector, 30 m away from the beam stop. Two upstream thin carbon targets, A1 and A2, located at 135 and 110 m from the detector center, respectively, provide additional small contributions to the ν_μ flux—also shown in Fig. 1(a). The main beam-related backgrounds (BRB) to the $\nu_\mu \rightarrow \nu_e$ search come from the intrinsic ν_e component of the beam, shown in Figs. 1(b) and 1(c). The flux from $\pi^+ \rightarrow e^+ \nu_e$ DIF is suppressed by the branching ratio of 1.23×10^{-4},

while the flux from $\mu^+ \rightarrow e^+ \nu_e \overline{\nu}_\mu$ DIF is suppressed by the longer μ lifetime and the kinematics of the three-body decay. The neutrino flux calculations are described in detail in Ref. [2] and yield a systematic error of 15% for the ν_μ DIF flux, confirmed by our measurement of the well understood $\nu_\mu\ ^{12}C \rightarrow \mu^- {}^{12}N_{gs}$ exclusive reaction [3]. The data discussed here correspond to 14 772 Coulombs of protons on target (POT) during the years 1993 (1787 C), 1994 (5904 C), and 1995 (7081 C). The beam duty factor—defined as the ratio of data collected with beam on to that with beam off—has a weighted average of 0.07.

The LSND apparatus [4], consists of a steel tank filled with 167 metric tons of liquid scintillator and viewed by 1220 uniformly spaced 8″ Hamamatsu photomultiplier tubes (PMT). The scintillator medium consists of mineral oil (CH_2) with a small admixture (0.031 g/l) of butyl-PBD. This allows the detection of both Čerenkov and isotropic scintillation light, so that the on-line reconstruction software provides robust particle identification (PID) for electrons, along with the event vertex and direction. The electronics and data acquisition (DAQ) systems were designed to detect and record related events separated in time. Despite 2.0 kg/cm² shielding above the detector tunnel, there remains a large background to the oscillation search due to cosmic rays. This background is highly suppressed by a veto shield [5], which provides both passive and active shielding. The veto system is viewed by 292 uniformly spaced 5″ EMI PMTs.
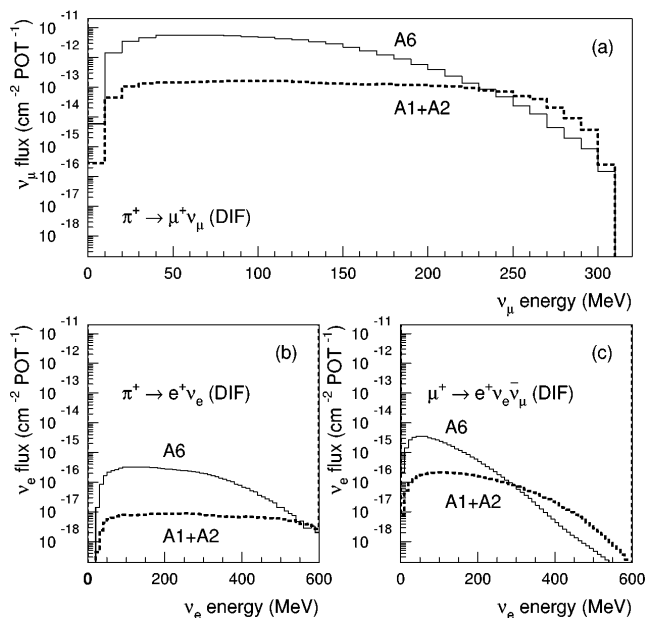

FIG. 1. Calculated ν_μ and ν_e DIF fluxes at the detector center from the A6 target (solid histograms) and from the A1 + A2 targets (dashed histograms).

A GEANT-based Monte Carlo (MC) is employed to simulate interactions in the LSND tank and the response of the detector system. The electron simulation is calibrated below 52.8 MeV using Michel electrons from the decay of stopped cosmic-ray muons and then extrapolated into the DIF energy range. The MC data set used to calculate electron selection efficiencies in the DIF analysis (DIF-MC) uses the calculated ν_μ flux, 100% $\nu_\mu \rightarrow \nu_e$ transmutation, and the $\nu_e C \rightarrow e^- X$ cross section calculated in the CRPA model [6,7].

Candidate events for $\nu_\mu \rightarrow \nu_e$ oscillation from the DIF ν_μ flux consist of a single, isolated electron (from the $\nu_e C \rightarrow e^- X$ reaction) in the energy range 60–200 MeV. The lower limit is chosen to be well above the end point of the Michel electron spectrum (52.8 MeV) to avoid backgrounds induced by cosmic-ray muons and beam-related ν_μ and $\bar{\nu}_\mu$ events. The upper limit of 200 MeV is the energy above which the beam-off background rates increase, and the expected signal becomes much attenuated. The analysis relies solely on electron PID in an energy regime for which no control sample is available.

A preliminary selection was made to arrive at an initial data sample. The electron PID parameters used in the DAR analysis [1] retain high efficiency (98.1±1.7)%, but have limited background rejection in the DIF energy range. New PID parameters developed for this analysis are used in the final event selection as described below. To reduce the cosmic-ray muon related background several cuts are made. First the veto shield is required to have less than four active PMTs. Second, the events must be reconstructed within the $d > 35$ cm fiducial volume. Finally, space-time and multiplicity correlations between the current event and its past/future neighboring events

eliminate cosmic-ray muons not vetoed by the DAQ. These cuts have an overall efficiency of (82.4 ± 2.7)% for electrons in the DIF energy range.

The event reconstruction and PID techniques used in the DIF analysis were developed to utilize fully the capabilities of the LSND apparatus. The basis for the reconstruction is a simple single track event model, parametrized by the track starting position and time, direction, and energy. For any given event, the expected photon intensities and arrival times are calculated from these parameters at all PMTs. A likelihood function that relates the *measured* PMT charge and time values to the *predicted* values is used to determine the best possible event parameters and also provides PID. Two analyses were performed, sharing basic goals, but differing in approach and parametrizations [8].

The essential goal of both analyses is to select events consistent with DIF candidate electrons, while eliminating remaining backgrounds from cosmic-ray interactions, including neutrons and photons. The electron identification relies primarily on the differences in the timing characteristics of the components of light produced in the event: scintillation light, and Čerenkov light, both direct and rescattered—Figs. 2(a) and 2(b). Furthermore, the event likelihood fitting returns also the fraction of direct Čerenkov light in the event, which provides excellent rejection against neutrons—Fig. 2(c).

High energy γ rays, from π^0 produced by neutron interactions in the lead shielding of the veto system, enter the detector fiducial volume without leaving a veto signal. The charged particles resulting from their interactions in the liquid point predominantly into the detector volume and are difficult to distinguish from electrons from the $\nu_e C \rightarrow e^- X$ reaction on the basis of electron PID alone. The backwards projected track length to the edge of the detector volume S is used to remove these events, concentrated at low values of S—Fig. 2(d). Events with any veto hits in time with the event, and along the backward extrapolation of the track, are also rejected.

Finally, the electron events in the final DIF sample are required to have $\cos\theta_\nu < 0.8$, where θ_ν is the angle between the reconstructed direction and the incident neutrino beam. This greatly reduces the BRB from the forward-peaked $\nu_\mu e$ elastic scattering, while retaining a high efficiency for the DIF signal.

After applying all of the respective selection criteria, both analyses obtain a significant and consistent beam-related event excess. One analysis ends up with 23 beam-on events and 114 beam-off events (8.0 rescaled for the duty factor), which corresponds to 15.0 excess events. The other analysis ends up with 25 beam-on events and 92 beam-off events (6.4 rescaled), which corresponds to 18.6 excess events. Their efficiencies are 8.4% and 13.8%, respectively, calculated for the $d > 0$ fiducial volume.

As already mentioned, the main BRBs in the DIF oscillation search come from the intrinsic ν_e contamination in the beam. These backgrounds are calculated using the beam MC neutrino fluxes and the $\nu_e C$ cross section
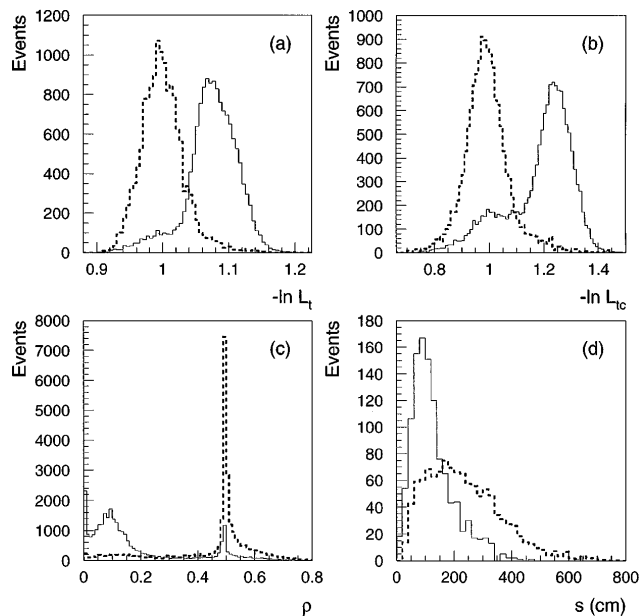
FIG. 2. Timing likelihoods for (a) the entire event and (b) the Čerenkov region only. (c) Čerenkov-to-scintillation density ratio ρ. (d) Projected track-length to the tank wall intersection. (a)–(c) correspond to all (beam on + off) DIF data after the preselection and (d) after all other cuts have been applied. All superimposed distributions (dashed) correspond to the DIF-MC simulation, normalized to the same areas.

calculated in the CRPA model. The $\nu_\mu e$ elastic scattering background from the ν_μ DIF flux is greatly reduced by requiring $\cos\theta_\nu < 0.8$. The last relevant background, $\pi^+ \to \mu^+ \nu_\mu$ DIF followed by $\nu_\mu C \to \nu_\mu C \pi^\circ$ coherent scattering, is calculated using the cross section in Ref. [9]. Backgrounds from the $\nu_\mu C \to \mu^- X$ reaction are negligible. The four relevant BRBs are summarized in Table I. The total BRBs calculated for the two analyses yield 4.5 and 8.5 events, respectively, which thus leaves a significant excess of events (10.5 and 10.1 events, respectively) above the expectation from conventional processes. The probabilities that the number of expected background events (12.5/14.9) fluctuate up to the observed beam-on numbers (23/25) are 0.7×10^{-2} and 1.6×10^{-2}, respectively.

Since both analyses have low efficiencies, different reconstruction software, and different selection criteria,

the two samples need not necessarily be identical. Both the logical AND and OR of the two samples have been extensively studied in MC simulations and the results are consistent with the expectations. For the final DIF sample we elect to use the logical OR of the events. This minimizes the sensitivity of the measurement to uncertainties in the efficiency calculations, is less sensitive to statistical fluctuations, and yields a larger efficiency. Table II summarizes the final event samples for the individual analyses, their overlap (AND), and the final sample (OR).

In the following we interpret the observed event excess of the OR sample in terms of the simplest, two-generation mixing neutrino oscillations formalism. In this model the oscillation probability is given by

$$ P = \sin^2 2\theta \, \sin^2\left(1.27\Delta m^2 \frac{L}{E_\nu}\right), \qquad (1) $$

where θ is the mixing angle, Δm^2 (eV^2/c^4) is the difference of the squares of the masses of the appropriate mass eigenstates, L (m) is the distance from neutrino production to detection, and E_ν (MeV) is the neutrino energy. Since the distance to the source is ambiguous because of the presence of multiple beam targets (A1, A2, and A6), the energy distribution alone is used to determine the confidence levels (C.L.) in the ($\sin^2 2\theta$, Δm^2) parameter space. Figure 3 shows the 95% C.L. contours that result from the fit. This result is consistent with the previous LSND DAR result [1], shown superimposed in Fig. 3. The oscillation probability is $(2.6 \pm 1.0 \pm 0.5) \times 10^{-3}$, where the second error is systematic, as described below.

The neutrino cross sections and fluxes constitute the largest source of systematic uncertainty for the DIF analysis, estimated to be 10% and 15%, respectively. The error on the electron PID is 12% and thus the total systematic error for this analysis is 22%. Although our measurement of $\nu_e C$ scattering using the DAR ν_e flux agrees well with calculations [10], our measurement of the inclusive $\nu_\mu C$ cross section [3] is 45% below the CRPA calculation [7]. The ν_μ flux in the $\nu_\mu C$ measurement is the same as for this DIF oscillation analysis, and it is possible that the $\nu_e C$ cross section at these higher energies also is below the CRPA calculation. The total number of

TABLE I. Background estimates for the $\nu_\mu \to \nu_e$ oscillation search for the $d > 0$ fiducial volume, 9.2×10^{22} POT, and for electron energies between 60 and 200 MeV. These numbers are illustrative for an electron selection efficiency of 0.10, independent of energy. The actual efficiencies in the two analyses are slightly different and energy dependent.

Process	Flux ($\text{cm}^{-2}\text{POT}^{-1}$)	$\langle\sigma\rangle_\nu$ (10^{-40} cm^2)	Eff. (%)	Number of events
$\nu_e C \to e^- X (\mu \text{ DIF})$	3.8×10^{-14}	28.3	10.0	3.8
$\nu_e C \to e^- X (\pi \text{ DIF})$	8.3×10^{-15}	79.2	10.0	1.6
$\nu_\mu C \to \nu_\mu C \pi^\circ$	6.5×10^{-11}	1.6	6.0	0.3
$\nu_\mu e \to \nu_\mu e$	6.5×10^{-11}	0.00136	0.5	0.1
Total background				5.8

TABLE II. Comparison of results for the two analyses (labeled here as A and B), their logical AND and OR. All errors are statistical. BUB = beam-unrelated background.

Data set	Beam on/off	BUB	BRB	Excess	Eff. (%)	Osc. Prob. $(\times 10^{-3})$
A	23/114	8.0 ± 0.7	4.5 ± 0.9	10.5 ± 4.9	8.4	2.9 ± 1.4
B	25/92	6.4 ± 0.7	8.5 ± 1.7	10.1 ± 5.3	13.8	1.7 ± 0.9
AND	8/31	2.2 ± 0.3	3.1 ± 0.6	2.7 ± 2.9	5.5	1.1 ± 1.2
OR	40/175	12.3 ± 0.9	9.6 ± 1.9	18.1 ± 6.6	16.5	2.6 ± 1.0

beam-excess events, N_{XCS}, is in average given by

$$N_{\mathrm{XCS}} = \varepsilon\, \sigma\, (\Phi_{\nu_\mu} P_{\nu_\mu \to \nu_e} + \Phi_{\nu_e}), \qquad (2)$$

where ε is the PID efficiency, σ is the ν_eC cross section, and Φ_{ν_μ/ν_e} are the ν_μ/ν_e fluxes. The oscillation signal is proportional to the same product $(\varepsilon\,\sigma\,\Phi_{\nu_\mu})$ as the neutrino background, since Φ_{ν_e} is proportional to Φ_{ν_μ}. The effect of *lowering* the product $\varepsilon\,\sigma\,\Phi_{\nu_\mu}$ is to reduce the predicted BRB, which raises the observed oscillation signal. This effect can be seen more clearly if one extracts the oscillation probability $P_{\nu_\mu \to \nu_e}$ from Eq. (2) above:

$$P_{\nu_\mu \to \nu_e} = \frac{N_{\mathrm{XCS}}}{\varepsilon\,\sigma\,\Phi_{\nu_\mu}} - \frac{\Phi_{\nu_e}}{\Phi_{\nu_\mu}} = \frac{N_{\mathrm{XCS}}}{\varepsilon\,\sigma\,\Phi_{\nu_\mu}} - \mathrm{const.} \qquad (3)$$

Only by *raising* the product $\varepsilon\,\sigma\,\Phi_{\nu_\mu}$ is the oscillation signal decreased. However, the Fermi gas model ν_eC cross section, which is only 10% higher than the CRPA prediction, yields a strict upper bound for the cross section, as we discuss in Ref. [8]. In order to calculate conservative confidence regions, we allow the value of $\varepsilon\,\sigma\,\Phi_{\nu_\mu}$ to vary between 22% above to 45% below the calculated value. Only a symmetrical 22% systematic error is used in the oscillation probability.

We have described a search for $\nu_e\, C \to e^- X$ interactions for electron energies $60 < E_e < 200$ MeV. Two different analyses observe a number of beam-on events significantly above the expected number from the sum of conventional beam-related processes and cosmic-ray (beam-off) events. The probability that the 21.9 ± 2.1 estimated background events fluctuate into 40 observed events is 1.1×10^{-3}. The excess events are consistent with $\nu_\mu \to \nu_e$ oscillations with an oscillation probability of $(2.6 \pm 1.0 \pm 0.5) \times 10^{-3}$. A fit to the energy distribution events, assuming neutrino oscillations as the source of ν_e, yields the allowed region in the $(\sin^2 2\theta, \Delta m^2)$ parameter space shown in Fig. 3, consistent with the allowed region from the DAR search reported earlier by LSND. This $\nu_\mu \to \nu_e$ DIF oscillation search has completely different backgrounds and systematic errors from the $\overline{\nu}_\mu \to \overline{\nu}_e$ DAR oscillation search and provides additional evidence that both effects are due to neutrino oscillations.
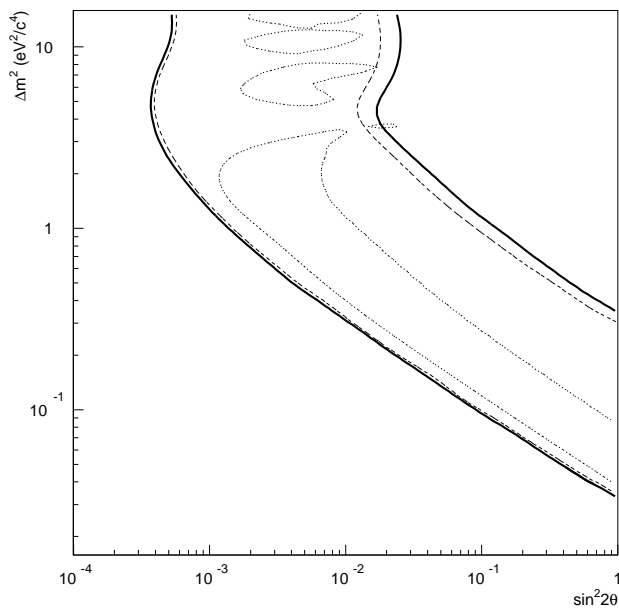
FIG. 3. The 95% C.L. region for the DIF $\nu_\mu \to \nu_e$ along with the favored regions from the LSND $\overline{\nu}_\mu \to \overline{\nu}_e$ DAR measurement (dotted contours). The dashed contour represents the 95% DIF C.L. for a symmetrical $\pm 19\%$ systematic error, assuming the ν_e C CRPA cross section with no errors.

[1] LSND Collaboration, C. Athanassopoulos *et al.,* Phys. Rev. C **54**, 2685 (1996); Phys. Rev. Lett. **77**, 3082 (1996).
[2] R. L. Burman, M. E. Potter, and E. S. Smith, Nucl. Instrum. Methods Phys. Res., Sect. A **291**, 621 (1990).
[3] LSND Collaboration, C. Athanassopoulos *et al.,* Phys. Rev. C **56**, 2806 (1997).
[4] LSND Collaboration, C. Athanassopoulos *et al.,* Nucl. Instrum. Methods Phys. Res., Sect. A **388**, 149 (1997).
[5] J. J. Napolitano *et al.,* Nucl. Instrum. Methods Phys. Res., Sect. A **274**, 152 (1989).
[6] E. Kolbe, K. Langanke, and S. Krewald, Phys. Rev. C **49**, 1122 (1994).
[7] E. Kolbe *et al.,* Phys. Rev. C **52**, 3437 (1995).
[8] LSND Collaboration, C. Athanassopoulos *et al.,* Report No. LA-UR-97-1998/UCRHEP-E191 (to be published).
[9] D. Rein and L. M. Sehgal, Nucl. Phys. **B223**, 29 (1983).
[10] LSND Collaboration, C. Athanassopoulos *et al.,* Phys. Rev. C **55**, 2078 (1997).